

# Estimating carbon pools in the shelf sea environment: reanalysis or model-informed machine learning?

Jozef Skákala

*Plymouth Marine Laboratory, Plymouth, UK,*

*National Centre for Earth Observation, Plymouth, UK.*

## Abstract

Shelf seas are important for carbon sequestration and carbon cycle, but shelf sea observations for carbon pools are often sparse, or highly uncertain. Alternative can be provided by reanalyses, but these are often expensive to run. We propose to use an ensemble of neural networks (i.e. deep ensemble) to learn from a coupled physics-biogeochemistry model the relationship between the directly observable variables and carbon pools. We demonstrate for North-West European Shelf (NWES) sea environment, that when the deep ensemble trained on a model free run simulation is applied to the NWES reanalysis, it is capable to reproduce the reanalysis outputs for carbon pools and additionally provide uncertainty information. We focus on explainability of the results and demonstrate potential use of the deep ensembles for future climate what-if scenarios. We suggest that model-informed machine learning presents a viable alternative to expensive reanalyses and could complement observations, wherever they are missing and/or highly uncertain.

## 1 Introduction

About 30% of carbon emitted into the atmosphere ends up absorbed by the ocean, where it circulates in multitude of organic and inorganic forms (Friedlingstein et al., 2024). The inorganic carbon gets used by autotrophs during photosynthesis, which is followed by material flows distributing it between many other pools, i.e. higher trophic level species (e.g. zooplankton, heterotrophic bacteria, fish), non-living organic forms (e.g. detrital, dissolved organic carbon), or the dissolved and particulate inorganic carbon (e.g. Emerson & Hedges (2008)). Part of the marine carbon gets eventually deposited to the sea bottom and sedimented, which helps to mitigate the anthropogenically driven climate change (Volk & Hoffert, 1985). Understanding the ocean carbon cycle is therefore essential for better understanding Earth system's response to atmospheric carbon emissions, both in the past and in the future projections. North-West European Shelf (NWES) comprising range of seas such as the North Sea, Celtic Sea, Irish Sea and the English Channel is of major relevance, since it is a highly biologically productive area with significant impact on carbon sequestration and transport (Borges et al., 2006; Jahnke, 2010; Legge et al., 2020).

A major source of information for the NWES are ocean surface observations derived from the satellite measurements. The biogeochemistry variable most typically de-

rived from satellite ocean color (OC) is the surface chlorophyll-*a* pigment concentrations (e.g. Groom et al. (2019)), which contain only indirect information about the NWES carbon pools. Variety of methods how to estimate carbon from satellite more directly have been proposed for a range of pools (Brewin et al., 2021), including total particulate organic carbon (POC, e.g. Evers-King et al. (2017); Le et al. (2018)), total phytoplankton carbon (e.g. Roy et al. (2017); Sathyendranath et al. (2020)), dissolved organic carbon (DOC, e.g. (Matsuoka et al., 2017; Laine et al., 2024)), and even indirect methods to estimate zooplankton carbon (e.g. Strömberg et al. (2009); Behrenfeld et al. (2019)) and of some bacterial species (Grimes et al., 2014; Racault et al., 2019) have been proposed. However these satellite algorithms have been most commonly developed for the global ocean, representing mostly open ocean conditions. Some shelf sea and coastal products exist for specific pools (e.g. DOC, Mannino et al. (2008); Matsuoka et al. (2017)), but have been developed for areas far from the NWES. Thus, apart of the relatively high uncertainty associated with many of those products, they might not be particularly suitable for the NWES. Beyond these satellite products the only available observations are in situ measured data. These cover quite well specific variables related to dissolved inorganic carbon (DIC), such as CO<sub>2</sub> fugacity and partial pressure (Bakker et al., 2014), but beyond those the in situ data are too sparse and limited to provide us with a more detailed understanding of the NWES carbon pools (for more general overview of in situ observational capacity in marine biogeochemistry see w.g. Telszewski et al. (2018)).

A more comprehensive picture is provided by the marine biogeochemistry models (Wakelin et al., 2012), but those can have on NWES large biases and uncertainties (e.g. for discussion see Skákala et al. (2022, 2024)). A compromise between the limited observations and imperfect models is the NWES Copernicus reanalysis (Kay et al., 2019, 2021), which constrains the model mostly with satellite observations (e.g. from OC, Sathyendranath et al. (2019)) and simultaneously delivers a range of outputs for the carbon pools. However producing reanalyses is computationally expensive especially for high-complexity biogeochemistry models and to keep the computational cost under control many simplifications are being adopted. These include constraining directly only biogeochemistry variables closely related to the OC product, i.e. phytoplankton biomass, with all other variables (e.g. the non-phytoplankton carbon pools) constrained only through the model dynamical adjustment (Skákala et al., 2018).

In this paper we propose an alternative: in line with the spirit of satellite retrieval algorithms we use a machine learning (ML) model to learn the relationship between the more directly observable variables from the satellite (such as sea surface temperature, OC derived size-class chlorophyll-*a*) and the unobserved carbon pools, but in our case the relationship is learned directly from the underlying NWES coupled physics-biogeochemistry model. In the coupled model such relationship emerges from a plethora of simulated processes, ranging from hydrodynamics to complex ecosystem interactions. Using the coupled model to inform the machine learning has several advantages: (i) there is no shortage of training data, i.e. the map from the observable variables to the carbon pools can be learned from the existing free run simulations, providing gap-free and abundant outputs, (ii) the coupled model is specifically calibrated for the NWES domain, and (iii) any carbon pool outputted by the model can be in theory predicted, including vertical distributions. The disadvantage of this approach is the assumption that the model-simulated relationship between the established satellite-observed variables (together with a range of model forcing data) and the derived carbon pools is sufficiently realistic. However, it can be argued that similar assumption is effectively used in the NWES reanalysis itself, so our approach just follows the logic applied in the reanalysis, but avoids the computational cost associated with it.

In this paper we demonstrate that a reasonably simple neural network (NN) can successfully learn from the operationally used physics-biogeochemistry model for the NWES how to derive range of surface carbon pools from several observable variables, forcing data and structural variables, such as latitude and longitude. When applied to the reanalysis inputs rather than the model free run it was trained on, the NN can reproduce well the ocean surface carbon pools from the reanalysis. We will produce insights into explainability of these results and discuss some interesting applications, such as running lightweight future climate what-if scenarios with such ML models.

## 2 Methodology

### 2.1 The physics-biogeochemistry coupled model

The model used in NWES Copernicus reanalysis (Kay et al., 2019, 2021) that we are emulating in this study is the physical model Nucleus for European Modelling of the Ocean (NEMO, Madec et al. (2015)), coupled to European Regional Seas Ecosystem Model (ERSEM, Baretta et al. (1995); Butenschön et al. (2016)) through Framework for Aquatic

Biogeochemical Models (FABM, Bruggeman & Bolding (2014)). The NEMO ocean physics component is a finite difference, hydrostatic, primitive equation ocean general circulation model, here used with a 7km (AMM7) NWES configuration using the terrain following  $z^*-\sigma$  coordinates with 51 vertical layers (O'Dea et al., 2017; Siddorn & Furner, 2013). ERSEM is a high complexity ecosystem model representing elemental cycles of carbon, nitrogen, phosphorus and silicon using variable stoichiometry. It represents four phytoplankton functional types (PFTs) which are mostly size-based (diatoms, nanophytoplankton, microphytoplankton and picophytoplankton), zooplankton in three functional types (mesozooplankton, microzooplankton and heterotrophic nanoflagellates) and as a decomposer it includes heterotrophic bacteria (Butenschön et al., 2016). The non-living organic matter is represented in three detrital forms (large, medium-size, small) and three forms of dissolved organic matter (labile, semi-refractory and refractory) (Butenschön et al., 2016). ERSEM uses variable stoichiometry representing biomass in carbon, nitrogen, phosphorus, for phytoplankton also chlorophyll and in case of diatoms also silicon. ERSEM includes carbonate system as per Artioli et al. (2012), representing dissolved inorganic carbon (DIC) and total alkalinity as two independent state variables (from which one can derive pH and pCO<sub>2</sub> as diagnostic variables).

## 2.2 The multi-decadal reanalysis

The capability of the ML model to predict carbon pools using observational data as inputs was subsequently tested on a data-set provided by Copernicus multi-decadal reanalysis (Kay et al., 2019, 2021). The reanalysis is based on the same NEMO-FABM-ERSEM model, constraining the model run through daily assimilation of SST from European Space Agency (ESA) Climate Change Initiative (CCI) v1.1 product, in situ SST from International Comprehensive Ocean-Atmosphere Data Set (ICOADS), temperature and salinity profiles from EN4 data (Good et al., 2013), and PFT (log-)chlorophyll from ESA CCI v3.1 data (Sathyendranath et al., 2019). The data are assimilated using NEMOVAR (Mogensen et al., 2012), based on 3DVar approach similar to the one described in King et al. (2018); Skákala et al. (2018). Within ERSEM the assimilation of PFT chlorophyll-*a* updates only the PFT biomass (all components chlorophyll-*a*, carbon, nitrogen, phosphorus, silicon), based on the forecast stoichiometry. The remaining ERSEM variables are unconstrained by the assimilation, and their values change only during the subsequent model simulation through the dynamical adjustment.

The reanalysis carbon can be validated with independent data, wherever they are available. For the relatively abundant ICES pCO<sub>2</sub> data-set this was already done in Kay et al. (2021), demonstrating a good skill. We have done here an additional comparison of the reanalysis outputs with OC-CCI v4.2 satellite product for the total POC (Stram-ski et al., 2008; Evers-King et al., 2017), comprising aggregate carbon of phytoplankton, zooplankton, detritus and bacteria pools. The results are shown in Fig.A1 of the Appendix. They indicate that the POC distributions are reasonably comparable between the reanalysis and satellite-derived product with some overall negative biases of the reanalysis. Satellite-derived DOC from Laine et al. (2024) was also available, unfortunately DOC was not outputted by the reanalysis and could not be compared to the satellite observations. However issues (major positive biases in hundreds of percents of the observed values) with ERSEM DOC have been found (Clark et al., 2025) and have been confirmed here (not shown). Although DOC pool is included here to demonstrate the ML capability to learn it from the model, it is recognized that as an end-product it would likely have at this stage only limited value.

### 2.3 The machine learning model

The NEMO-FABM-ERSEM configuration providing the simulations for the training data has been described in Skákala et al. (2020). The simulation delivering the training data-set has been performed in Higgs et al. (2023) for a 5 year period 2016-2020, providing daily outputs for all the relevant carbon pools. The training data have been produced by coarsening the simulation outputs (through averaging) to a 10-day temporal scale and 35km (5x5 model pixel) spatial scale. These coarser scales were chosen to reduce the data redundancy/duplication due to their spatial and temporal correlations, improving the efficiency of the training and validation of the ML model.

We have used feed-forward neural network (NN) model based on Tensorflow Keras library, with three hidden layers and approximately 2200 neurons. The NN model used Adam optimizer, root mean squared cost function and random initialization of weights based on normal distribution. To reduce overfitting and optimize performance we have used dropout function with 30% of neurons randomly switched off at each learning step. The 2016-2020 data-set was split into the 2016-2019 period used as the training data-set and 2020 year for validation. We have used a 15-member ensemble of the NN model realizations (i.e. deep ensemble) to boost the performance and introduce some estimate

of (mostly epistemic) uncertainty. The ensemble members were naturally distinguished through the random model parameters, such as weight initialization, dropout function and other random procedures, such as splitting the training data into batches (batch size of 32 was used). Prediction was taken from the ensemble mean and uncertainty was evaluated as the ensemble standard deviation.

The deep ensemble used as features (i) observable variables, i.e. sea surface PFT chlorophyll, sea surface temperature (SST) and sea surface salinity, (ii) “structural” inputs, i.e. latitude and longitude, bathymetry and the day of the year, (iii) atmospheric inputs, i.e. incoming short-wave radiation, surface wind speed, and (iv) collection of riverine discharge data processed as described in Banerjee & Skákala (2025). The deep ensemble predicted at each coarsened (35km) grid location a number of carbon pools in the output layer, i.e. for (i) total surface zooplankton, (ii) total surface detritus, (iii) total surface dissolved organic matter, (iv) surface heterotrophic bacteria, (v) surface dissolved inorganic matter, and vertically averaged values for all these pools except for zooplankton.

The performance of the relatively “lightweight” NN model design could be potentially improved by utilizing spatial and temporal structure among the model inputs, e.g. through more sophisticated architectures such as convolutional NN (Li et al., 2021), or Long-Short Term Memory (LSTM, Hochreiter & Schmidhuber (1997); Yu et al. (2019)) NNs. However, although here the model was tested on a gap-free reanalysis inputs for SST, sea surface salinity and PFT chlorophyll, the real purpose of such NN models would be to replace the reanalysis and predict carbon pools directly from the satellite data, which have many gaps due to cloud cover and atmospheric disturbances. The simpler architecture, such as feed-forward NN was thus found preferable, since it is more adaptable to situations with irregular data with gaps, predicting carbon pools locally, wherever the model inputs are present.

## 2.4 Experiments and validation metrics

The model performance on the independent data produced by the reanalysis was evaluated by comparing the spatial distributions of 2016-2020 time-averaged reanalysis and predicted carbon pools, indicating the overall biases of the prediction. A separate metrics of Bias-Corrected Root-Mean Square Difference (BC-RMSD) was applied, de-

fined as

$$\text{BC-RMSD} = \sqrt{\langle (X_1 - X_2 - (\langle X_1 \rangle - \langle X_2 \rangle))^2 \rangle}, \quad (1)$$

where  $X_1, X_2$  are the two compared data-sets. The BC-RMSD % improvement generated by data 1 (with BC-RMSD<sub>1</sub>) relative to data 2 (with BC-RMSD<sub>2</sub>) is defined as

$$\text{BC-RMSD}_{imp} = 100 \cdot \frac{\text{BC-RMSD}_1 - \text{BC-RMSD}_2}{\text{BC-RMSD}_2}. \quad (2)$$

We have used the deep ensemble to predict hypothetical what-if scenarios. Two scenarios were chosen for the ensemble prediction: (i) one where PFT chlorophyll is scaled down from the 2016-2020 reanalysis value gradually to zero, maintaining the same PFT community structure and spatio-temporal distributions as in the reanalysis, (ii) another where the ratio of large phytoplankton (sum of diatoms and dinoflagellates) to total phytoplankton was gradually scaled from the 2016-2020 reanalysis down to zero, but maintaining the same total chlorophyll concentration and spatio-temporal distributions as in the 2016-2020 reanalysis. In both cases the NN model inputs other than PFT chlorophyll were kept the same as in the reanalysis. These scenarios (defined by the NN inputs) were motivated by certain aspects of future climate projections for the NWES (Wakelin et al., 2015), but are obviously major simplifications, e.g. there is no guarantee that the scenarios are sufficiently self-consistent, as they did not come from a model simulation.

### 3 Results

The deep ensemble performance on validation data is very good, with  $R^2$  of the surface pools between 0.83 and 0.89, and for the vertically averaged pools in the 0.9-0.92 range, except for the vertically averaged DIC, where it was lower ( $R^2 = 0.68$ ). The Fig.1 shows the performance of the deep ensemble on both, 2016-2020 free run training and validation (training-validation) data (comparing first and second rows), and the reanalysis, test data (comparing third and fourth rows). The Figure compares the deep ensemble biases, as well as biases among the free run (first row) and the reanalysis (third row). It is demonstrated that except for DIC (fifth column) the surface concentrations of the carbon pools in the reanalysis are substantially lower than in the free run. This is due to reduction in phytoplankton concentration caused by the assimilation of satellite data (see Skákala et al. (2018, 2020)), that propagates to the other organic carbon pools. The deep ensemble, trained on the free run data, is capable to pick this pattern, as can be

seen by comparing the rows three and four in Fig.1. In fact for detrital matter the deep ensemble predicts larger reduction in detritus than the reanalysis, whilst for zooplankton and bacteria the reduction is slightly lower, but the deep ensemble predicted values are in all cases reasonably close to the reanalysis.

The comparison in Fig.1 is complemented by BC-RMSD<sub>imp</sub> metrics from Fig.2, showing the % improvement in BC-RMSD when comparing the BC-RMSD of the deep ensemble prediction using the reanalysis inputs with the BC-RMSD of the free run. The BC-RMSD is in both cases calculated separately for each spatial location and measured relative to the reanalysis data. Fig.2 clearly demonstrates that the deep ensemble prediction from reanalysis inputs substantially outperforms the free run in all surface carbon pools except for DIC (DOC could not be compared due to the lack of reanalysis output). This means it is preferable to use the deep ensemble prediction of these carbon pools than running the free model simulation, and this is true not just for the time-averaged values (Fig.1), but also for the time-series hidden behind the time-averages (Fig.2).

Curiously deep ensemble failed to improve the vertically averaged pools (not shown here). This can be understood based on SHapley Additive exPlanations (SHAP, Lundberg & Lee (2017)) analysis shown in Fig.A2-A3 of the Appendix. Using SHAPS it has been observed that for the vertically averaged variables the structural inputs (coordinates, bathymetry and annual day) are more important than they are for the surface variables (Fig.A2-A3 of the Appendix demonstrates this for heterotrophic bacteria carbon and for DOC). High importance of structural variables suggests that the deep ensemble mostly learned the free run climatology of the vertically averaged variables, showing too little flexibility when moving towards reanalysis. We have tried improving upon the structure of the NN models by including time-lagged features, to potentially represent longer time-scales associated with the vertically averaged variables, but there was no marked improvement to the results (not shown here). Finally, the SHAP analysis has shown consistently across all the carbon pools that the two most important groups of variables are oceanic inputs (SST, salinity, PFT chlorophyll) and structural variables, with atmospheric variables being less important and riverine discharge the least important.

There are two main reasons why the deep ensemble could have failed when predicting the carbon pools from the reanalysis: (i) the NN inputs provided by the reanalysis



**Figure 1.** The 2016-2020 average values of different estimated carbon pools comprising ocean surface concentrations of detritus (first column), DOC (second column), zooplankton (third column), heterotrophic bacteria (fourth column) and DIC (fifth column). Compared are the NEMO-FABM-ERSEM free run providing the training and validation data (first row), the prediction of these data by the mean of the deep ensemble (second row), the Copernicus reanalysis concentrations from Kay et al. (2021) (third row) and the analogue of these reanalysis concentrations predicted by the mean of the deep ensemble from the reanalysis inputs (fourth row). In the bottom, fifth row the panels show the uncertainties of the estimated concentrations from the fourth row obtained as the standard deviation of the deep ensemble averaged in time. The reanalysis DOC is masked, since it was not available in the reanalysis outputs.

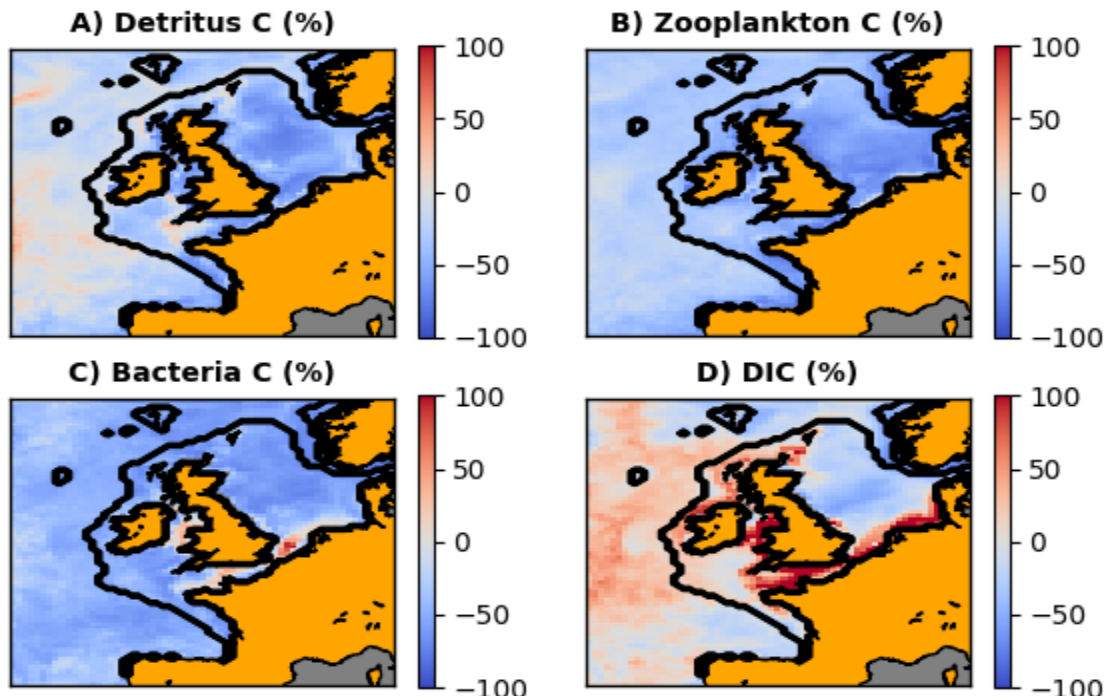


**Figure 2.** The relative percentage (%) improvement at ocean surface captured by BC-RMSD<sub>imp</sub> (see Eq.2) as measured relatively to the reanalysis. The blue color means that the deep ensemble mean outperforms the free run and the red color means that it performs worse than the free run. The BC-RMSD's are calculated across the 2016-2020 period.

were too far from the data seen by the NN in the training process, (ii) the inherent relationship between the NN model inputs and the predicted NN outputs, learned by the NN, differs between the reanalysis and the model free run. Fig.3 shows that the reanalysis inputs were not far from what the deep ensemble has seen during training and validation, as their distance from the training and validation data-set was on average no significantly larger than the typical distance between the data-points within the training and validation data-set. The point (ii) is a little bit more tricky: although the relationship between NN model inputs and the predicted outputs in the reanalysis is provided via the dynamical adjustment of the same biogeochemistry model, whose free run was used to train the NN, there is no guarantee that the map from the NN inputs to the outputs within the reanalysis will not get distorted by the impact of assimilation. An interesting insight is provided by Fig.4 showing the dependence of surface carbon pools on chlorophyll-*a*. Although the dependency plotted in Fig.4 is a major simplification of the true function learned by the deep ensemble, it indicates that the functions between NN inputs and detritus and zooplankton carbon pools might significantly differ between the model free run and the reanalysis. It is also notable that for zooplankton and detritus the deep ensemble predicts similar functional dependence as the free run. This suggests that the deviation between the deep ensemble prediction and the reanalysis in Fig.4:A,C is due to differences in those functional dependencies between the free run and the reanalysis, i.e. deep ensemble using the function it learned in the free run to create predictions on the space of reduced chlorophyll-*a* concentrations from the reanalysis. Interestingly the same is less true for the heterotrophic bacteria carbon and the DOC (Fig.4:B,D).

It is tempting to use the lightweight NN-based emulators to simulate a wide range of what-if scenarios, something hard to do with computationally expensive precess-based models. The future climate projections for the NWES indicate important changes to a range of variables included as inputs in the NN (Wakelin et al., 2015). This includes decline in near-surface primary production and therefore phytoplankton biomass, and changes to phytoplankton community structure, with increased proportion of smaller size-classes in the phytoplankton community. Both these changes are thought to be primarily driven through the increased thermal stratification of the ocean, cutting off the nutrients from the ocean surface (Wakelin et al., 2015). In Fig.5 we plot the response of ocean surface carbon pools as predicted by the deep ensemble to such changes in the surface phytoplankton. The functional relationships from Fig.5:A can be easily understood, as they

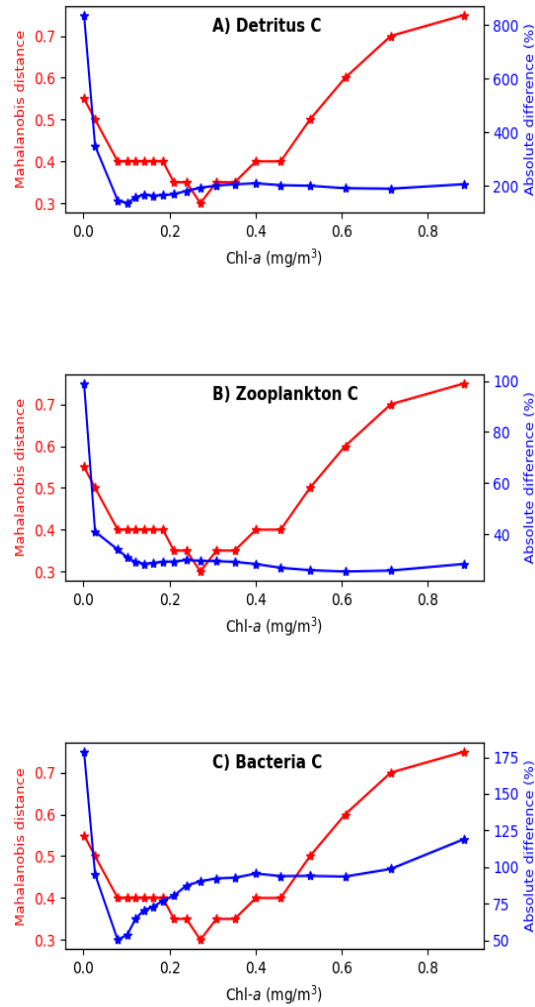


**Figure 3.** The red line in each plot shows Mahalanobis distance (Chandra, 1936; Ghorbani, 2019) of the reanalysis inputs relative to the training and validation (training-validation) data calculated as follows: Chlorophyll-*a* from the reanalysis (x-axis) was split into 20 quantiles and for each quantile we calculated median Mahalanobis distance between reanalysis and the training-validation data-set. Then we identified where (into which quantile) this median falls within the distribution of Mahalanobis distances within the training-validation data-set itself (calculated as distribution of Mahalanobis distances of the training-validation data from the training-validation data-set itself). The red y-axis then shows those quantiles on the 0-1 range of values, i.e. if the value is 0.5 it means that the median distance between reanalysis point and training-validation data-set was the same as the median distance among the training-validation data. If it is larger than 0.5, than the reanalysis points were generally further from the training-validation data-set than the average and vice versa. The blue line shows for the same quantiles the deep ensemble prediction skill measured against the reanalysis through mean absolute difference relative to the mean concentration (in %).

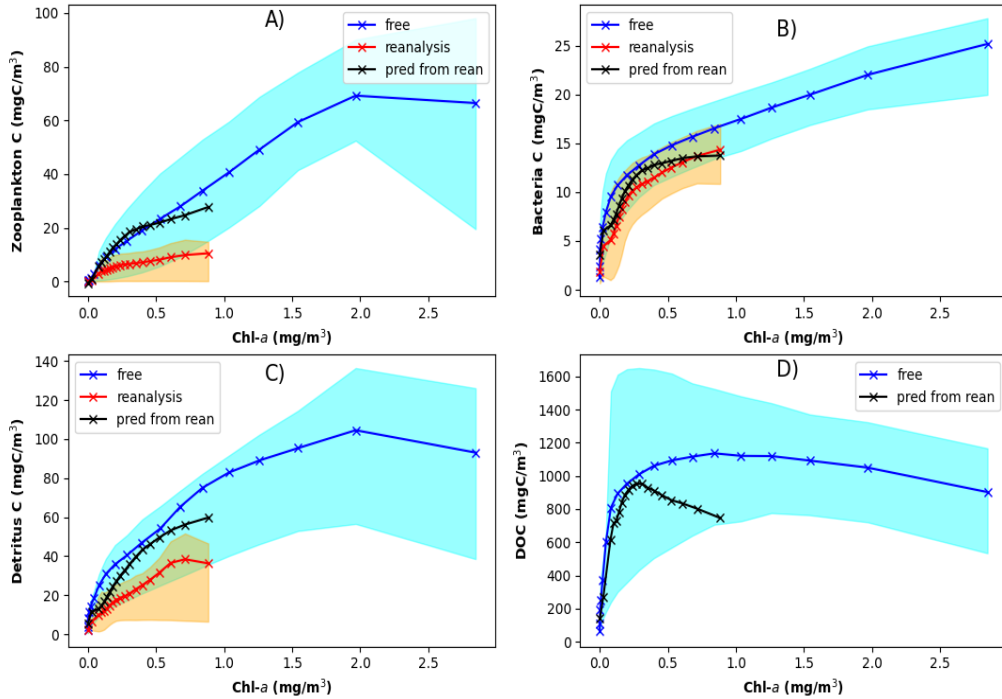


**Figure 4.** On the x-axis we show phytoplankton surface chlorophyll-*a* concentrations (in  $\text{mg}/\text{m}^3$ ). The markers on the lines show on the x-axis 20 quantiles into which the total chlorophyll-*a* distribution was split. On the y-axis the markers show for each chlorophyll-*a* quantile the median values of the different carbon pools: zooplankton (A), heterotrophic bacteria (B), detritus (C) and DOC (D). The shaded colors show the spread of the values for each carbon pool across each chlorophyll-*a* quantile, i.e. the spread is calculated from the model free run and defined for each carbon pool as two quartiles around its (model free run) median value for each chlorophyll-*a* quantile. The different markers/lines account for the model free run, reanalysis and the deep ensemble prediction using reanalysis as inputs.

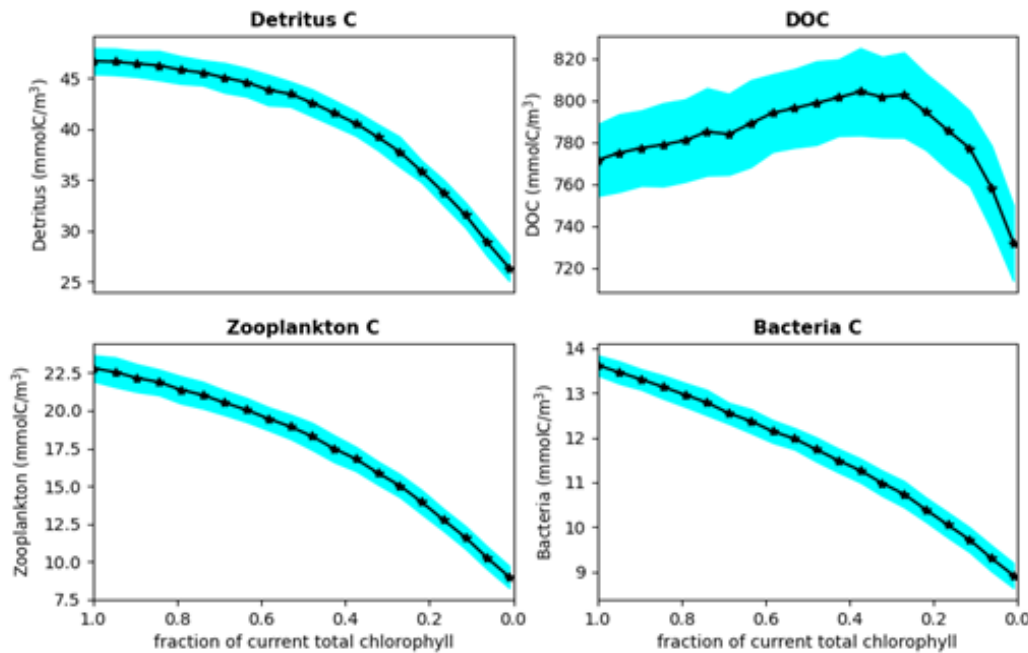
just indicate an overall decline of organic carbon pools with the decline of phytoplankton biomass. However, the dependence of the same ocean surface carbon pools on the ocean surface phytoplankton community structure (Fig.5:B) is in some cases more complex. Whilst the surface detrital carbon monotonically increases with reduced large-size phytoplankton presence likely due to decrease in sinking rates and carbon export, the non-monotonous changes in DOC and zooplankton carbon pools are likely influenced by the changes in their own functional type compositions as a function of the modified phytoplankton community structure.

There are many reasons to be cautious about the results presented in Fig.5. Even though the what-if scenario input features did not have anomalously large Mahalanobis distance from the training data (not shown here), one can raise serious doubts about how the statistical relationship learned by the deep ensemble in the model hindcast translates into a hypothetical future climate. We have tested this by a series of 1D simulations using Generalised Ocean Turbulence Model (GOTM, Burchard et al. (1999)) coupled to ERSEM through FABM. In those simulations we reduced nutrients by relaxing them towards lowered climatology values, triggering decrease in primary production and phytoplankton in the 1D model. We have trained a deep ensemble based on the simulation data where nutrients were not reduced and we analysed how well the deep ensemble predicts the carbon pools from the 1D simulations with reduced nutrients. These experiments (see Fig.6) suggest that the deep ensemble prediction has a persistent tendency to underestimate the impact of phytoplankton reduction on the carbon pools, with the underestimate becoming large as phytoplankton biomass is reduced. The 1D experiments would then nicely explain why the carbon pools in Fig.5 do not approach zero as the phytoplankton concentration vanishes. However, the deep ensemble was capable to do a decent job in estimating bacteria carbon changes until the phytoplankton biomass was reduced by more than 30% (Fig.6:D). This simple exercise shows that although similar what-if scenarios using deep ensembles should be taken with healthy suspicion, there might be specific cases where the prediction works well within a relatively wide range of scenarios.

#### 4 Conclusions and the next steps

In this work we have demonstrated that we can estimate surface carbon pools in the NWES using model-informed machine learning (ML), which could effectively replace

## A) Phytoplankton biomass changes



## B) Community structure changes

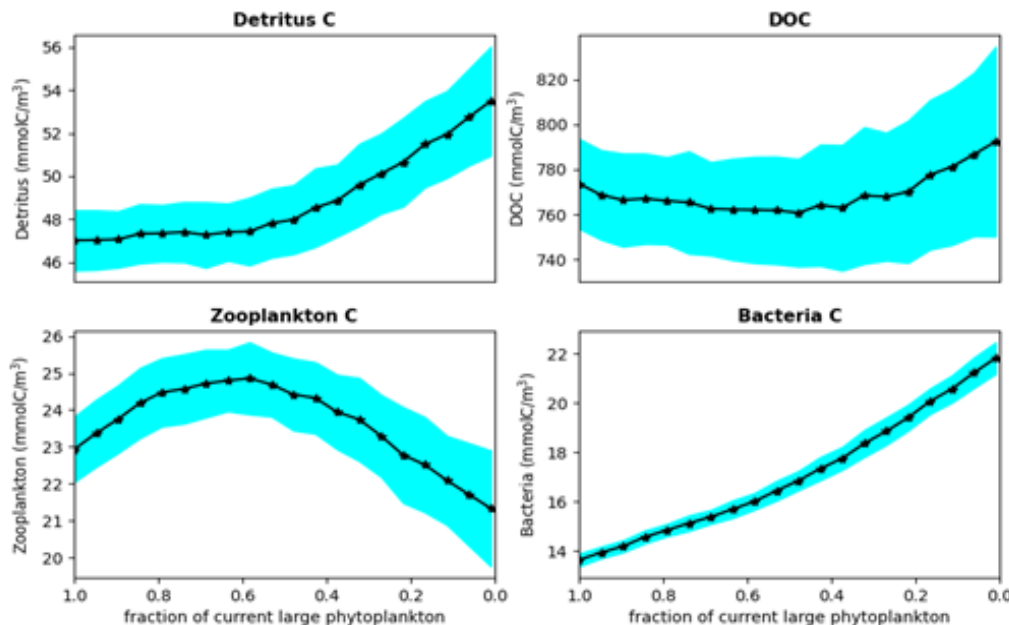


**Figure 5.** A) Deep ensemble predicted what-if scenario for how decline in phytoplankton biomass measured as a fraction of its present 2016-2020 reanalysis value (on [0-1] scale) maps into the estimated carbon pools. B) Similar what-if scenario for changes in the community structure measured by the ratio in chlorophyll-*a* biomass between macrophytoplankton (diatoms and dinoflagellates) and total phytoplankton, relative to the average reanalysis 2016-2020 ratio (again on a [0-1] scale). The shaded areas show in both cases the uncertainty derived from the deep ensemble standard deviation.

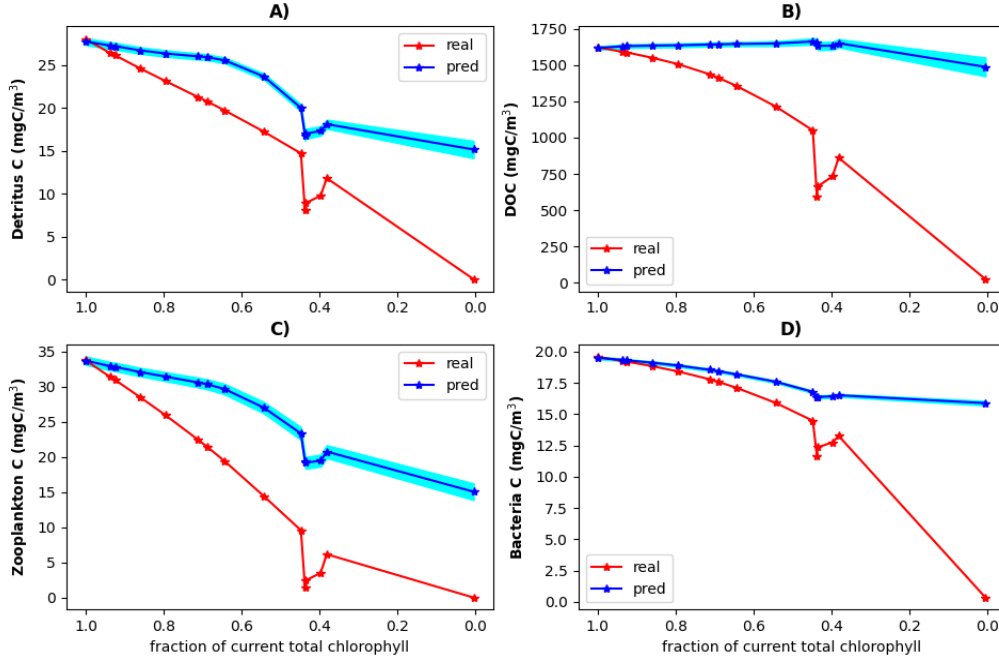


**Figure 6.** 1D experiments forced by nutrient relaxation to a state with reduced surface phytoplankton concentrations emulating changed climate. In red is the relationship between time-averaged total chlorophyll-a (x-axis) and time-averaged carbon pools (y-axis) from the 1D model runs. Each 1D simulation was run for 20 years with 5 years used as spin-up and 15 years used to calculate the averages for each "climate" state. The simulations were run at L4 location in the western English Channel with atmospheric forcing taken from real 2001-2020 data (hence the only forcing changing the climate state was the nutrient relaxation). In blue is deep ensemble prediction of the surface carbon pools, using the inputs from the 1D runs. The deep ensemble was trained on the simulation with the present state nutrients. The Figure shows how much is the deep ensemble capable to generalize from the current climate to different climate states.

reanalysis by a highly cost-effective emulator. The ML emulator can be trained on the free model runs, and then applied to derive those surface pools (and their uncertainties) directly from the observations. Such model-informed ML could complement the existing satellite algorithms in regions where they perform poorly, or for such carbon pools where they are non-existent, or highly uncertain.

As the surface carbon pools carry only limited information about carbon cycle, estimating vertical profiles of those pools is quite essential, e.g. to get answers to questions such as how much carbon is exported into the deep ocean. The approach adopted in this work was able to only learn the seasonal climatology of the vertically averaged carbon pools. This might be likely due to the relative simplicity of the ML design adopted and even though implementing time-lagged features did not seem to help, there is a chance that improvement can be made with more sophisticated models and longer data-sets. As part of increasing model complexity, one could also consider replacing the structural ML inputs with new flow-dependent features, e.g. capturing the underlying hydrodynamics. Such new features would however likely require using observations from profiles, significantly constraining the spatial domain where the ML model can be applied, or a 3D physical model run, making the applicability of the ML model significantly more demanding in terms of the required inputs into the model (relying on 3D hydrodynamic model runs).

Finally, other applications of the existing ML surface carbon prediction can be imagined, these include implementing assimilation of the ML-derived surface carbon alongside the currently assimilated variables, similarly to what was done with nitrate in Banerjee et al. (2025). If this was done “online” with the ML prediction cycled with the DA (see the discussion in Banerjee et al. (2025)) we could improve the speed with which the model adjusts itself to assimilation of standardly provided satellite data (such as OC chlorophyll-*a*). We suggest to explore these routes in the future.

**Acknowledgments:** This work was funded by the Horizon Europe project The New Copernicus Capability for Tropic Ocean Networks (NECCTON, grant agreement no.101081273). We also acknowledge support from the UK Natural Environment Research Council, including the single centre national capability programme – Climate Linked Atlantic Sector Science (CLASS, 379NE/R015953/1). I would like to thank David Ford and

Richard Renshaw for providing me with access to the Copernicus reanalysis data on the Met Office HPC MonSOON2 storage system MASS.

## References

Artioli, Y., Blackford, J. C., Butenschön, M., Holt, J. T., Wakelin, S. L., Thomas, H., ... Allen, J. I. (2012). The carbonate system in the north sea: Sensitivity and model validation. *Journal of Marine Systems*, 102, 1–13.

Bakker, D. C., Pfeil, B., Smith, K., Hankin, S., Olsen, A., Alin, S. R., ... others (2014). An update to the surface ocean co 2 atlas (socat version 2). *Earth System Science Data*, 6(1), 69–90.

Banerjee, D., & Skákala, J. (2025). Improved understanding of eutrophication trends, indicators and problem areas using machine learning. *Biogeosciences (in press)*. doi: doi.org/10.22541/essoar.171405637.76928549/v1

Banerjee, D., Skakala, J., & Ford, D. (2025). Combining machine learning with data assimilation to improve the quality of phytoplankton forecasting in a shelf sea environment. *submitted to QJRMS, arXiv:2508.02400*.

Baretta, J., Ebenhöh, W., & Ruardij, P. (1995). The european regional seas ecosystem model, a complex marine ecosystem model. *Netherlands Journal of Sea Research*, 33(3-4), 233–246.

Behrenfeld, M. J., Gaube, P., Della Penna, A., O'malley, R. T., Burt, W. J., Hu, Y., ... others (2019). Global satellite-observed daily vertical migrations of ocean animals. *Nature*, 576(7786), 257–261.

Borges, A., Schiettecatte, L.-S., Abril, G., Delille, B., & Gazeau, F. (2006). Carbon dioxide in european coastal waters. *Estuarine, coastal and shelf science*, 70(3), 375–387.

Brewin, R. J., Sathyendranath, S., Platt, T., Bouman, H., Ciavatta, S., Dall'Olmo, G., ... others (2021). Sensing the ocean biological carbon pump from space: A review of capabilities, concepts, research gaps and future developments. *Earth-Science Reviews*, 217, 103604.

Bruggeman, J., & Boldig, K. (2014). A general framework for aquatic biogeochemical models. *Environmental modelling & software*, 61, 249–265.

Burchard, H., Boldig, K., & Villarreal, M. R. (1999). *Gotm, a general ocean turbulence model: Theory, implementation and test cases*. Space Applications Institute.

Butenschön, M., Clark, J., Aldridge, J. N., Allen, J. I., Artioli, Y., Blackford, J., ... others (2016). Ersem 15.06: a generic model for marine biogeochemistry and the ecosystem dynamics of the lower trophic levels. *Geoscientific Model Development*, 9(4), 1293–1339.

Chandra, M. P. (1936). On the generalised distance in statistics. In *Proceedings of the national institute of sciences of india* (Vol. 2, pp. 49–55).

Clark, J., Kay, S., Samuelsen, A., Conchon, A., Albernehe, S., Butenschon, M., ... Gregoire, M. (2025). Neccton: Technical specification of the pelagic lower trophic level products. *Zenodo*. doi: <https://doi.org/10.5281/zenodo.10057818>

Emerson, S., & Hedges, J. (2008). *Chemical oceanography and the marine carbon cycle*. Cambridge University Press.

Evers-King, H., Martinez-Vicente, V., Brewin, R. J., Dall'Olmo, G., Hickman, A. E., Jackson, T., ... others (2017). Validation and intercomparison of ocean color algorithms for estimating particulate organic carbon in the oceans. *Frontiers in Marine Science*, 4, 251.

Friedlingstein, P., O'sullivan, M., Jones, M. W., Andrew, R. M., Hauck, J., Landschützer, P., ... others (2024). Global carbon budget 2024. *Earth System Science Data Discussions*, 2024, 1–133.

Ghorbani, H. (2019). Mahalanobis distance and its application for detecting mul-

tivariate outliers. *Facta Universitatis, Series: Mathematics and Informatics*, 583–595.

Good, S. A., Martin, M. J., & Rayner, N. A. (2013). En4: Quality controlled ocean temperature and salinity profiles and monthly objective analyses with uncertainty estimates. *Journal of Geophysical Research: Oceans*, 118(12), 6704–6716.

Grimes, D. J., Ford, T. E., Colwell, R. R., Baker-Austin, C., Martinez-Urtaza, J., Subramaniam, A., & Capone, D. G. (2014). Viewing marine bacteria, their activity and response to environmental drivers from orbit: satellite remote sensing of bacteria. *Microbial ecology*, 67(3), 489–500.

Groom, S., Sathyendranath, S., Ban, Y., Bernard, S., Brewin, R., Brotas, V., ... others (2019). Satellite ocean colour: current status and future perspective. *Frontiers in Marine Science*, 6, 485.

Higgs, I., Skákala, J., Bannister, R., Carrassi, A., & Ciavatta, S. (2023). Ecosystem connections in the shelf sea environment using complex networks. *EGUphere*, 2023, 1–28.

Hochreiter, S., & Schmidhuber, J. (1997). Long short-term memory. *Neural computation*, 9(8), 1735–1780.

Jahnke, R. A. (2010). Global synthesis1. In *Carbon and nutrient fluxes in continental margins: A global synthesis* (pp. 597–615). Springer.

Kay, S., McEwan, R., & Ford, D. (2019). North west european shelf production centre northwestshelf\_analysis\_forecast\_bio\_004\_011, quality information document. *Copernicus Marine Environment Monitoring Service*.

Kay, S., McEwan, R., & Ford, D. (2021). North west european shelf production centre nwshelf\_multiyear\_bio\_004\_011. *CMEMS Report*, 3, 21.

King, R. R., While, J., Martin, M. J., Lea, D. J., Lemieux-Dudon, B., Waters, J., & O'Dea, E. (2018). Improving the initialisation of the met office operational shelf-seas model. *Ocean Modelling*, 130, 1–14.

Laine, M., Kulk, G., Jönsson, B. F., & Sathyendranath, S. (2024). A machine learning model-based satellite data record of dissolved organic carbon concentration in surface waters of the global open ocean. *Frontiers in Marine Science*, 11, 1305050.

Le, C., Zhou, X., Hu, C., Lee, Z., Li, L., & Stramski, D. (2018). A color-index-based empirical algorithm for determining particulate organic carbon concentration in the ocean from satellite observations. *Journal of Geophysical Research: Oceans*, 123(10), 7407–7419.

Legge, O., Johnson, M., Hicks, N., Jickells, T., Diesing, M., Aldridge, J., ... Burrows, M. T. e. a. (2020). Carbon on the northwest european shelf: Contemporary budget and future influences. *Frontiers in Marine Science*, 7, 143.

Li, Z., Liu, F., Yang, W., Peng, S., & Zhou, J. (2021). A survey of convolutional neural networks: analysis, applications, and prospects. *IEEE transactions on neural networks and learning systems*, 33(12), 6999–7019.

Lundberg, S. M., & Lee, S.-I. (2017). A unified approach to interpreting model predictions. *Advances in neural information processing systems*, 30.

Madec, G., et al. (2015). Nemo ocean engine.

Mannino, A., Russ, M. E., & Hooker, S. B. (2008). Algorithm development and validation for satellite-derived distributions of doc and cdom in the us middle atlantic bight. *Journal of Geophysical Research: Oceans*, 113(C7).

Matsuoka, A., Boss, E., Babin, M., Karp-Boss, L., Hafez, M., Chekalyuk, A., ... Bricaud, A. (2017). Pan-arctic optical characteristics of colored dissolved organic matter: Tracing dissolved organic carbon in changing arctic waters using satellite ocean color data. *Remote sensing of Environment*, 200, 89–101.

Mogensen, K., Balmaseda, M. A., Weaver, A., et al. (2012). The nemo var ocean data assimilation system as implemented in the ecmwf ocean analysis for system 4.

O'Dea, E., Furner, R., Wakelin, S., Siddorn, J., While, J., Sykes, P., ... Hewitt, H. (2017). The co5 configuration of the 7 km atlantic margin model: large-scale biases and sensitivity to forcing, physics options and vertical resolution. *Geoscientific Model Development*, 10(8), 2947.

Racault, M.-F., Abdulaziz, A., George, G., Menon, N., C, J., Punathil, M., ... others (2019). Environmental reservoirs of vibrio cholerae: challenges and opportunities for ocean-color remote sensing. *Remote Sensing*, 11(23), 2763.

Roy, S., Sathyendranath, S., & Platt, T. (2017). Size-partitioned phytoplankton carbon and carbon-to-chlorophyll ratio from ocean colour by an absorption-based bio-optical algorithm. *Remote Sensing of Environment*, 194, 177–189.

Sathyendranath, S., Brewin, R. J., Brockmann, C., Brotas, V., Calton, B., Chuprin, A., ... others (2019). An ocean-colour time series for use in climate studies: The experience of the ocean-colour climate change initiative (oc-cci). *Sensors*, 19(19), 4285.

Sathyendranath, S., Platt, T., Kovač, Ž., Dingle, J., Jackson, T., Brewin, R. J., ... Bouman, H. A. (2020). Reconciling models of primary production and photoacclimation. *Applied Optics*, 59(10), C100–C114.

Siddorn, J., & Furner, R. (2013). An analytical stretching function that combines the best attributes of geopotential and terrain-following vertical coordinates. *Ocean Modelling*, 66, 1–13.

Skákala, J., Bruggeman, J., Brewin, R. J., Ford, D. A., & Ciavatta, S. (2020). Improved representation of underwater light field and its impact on ecosystem dynamics: a study in the north sea. *Journal of Geophysical Research: Oceans*, e2020JC016122.

Skákala, J., Bruggeman, J., Ford, D., Wakelin, S., Akpinar, A., Hull, T., ... others (2022). The impact of ocean biogeochemistry on physics and its consequences for modelling shelf seas. *Ocean Modelling*, 172, 101976.

Skákala, J., Ford, D., Brewin, R. J., McEwan, R., Kay, S., Taylor, B., ... Ciavatta, S. (2018). The assimilation of phytoplankton functional types for operational forecasting in the northwest european shelf. *Journal of Geophysical Research: Oceans*, 123(8), 5230–5247.

Skákala, J., Ford, D., Fowler, A., Lea, D., Martin, M. J., & Ciavatta, S. (2024). How uncertain and observable are marine ecosystem indicators in shelf seas? *Progress in Oceanography*, 224, 103249.

Stramski, D., Reynolds, R. A., Babin, M., Kaczmarek, S., Lewis, M. R., Röttgers, R., ... others (2008). Relationships between the surface concentration of particulate organic carbon and optical properties in the eastern south pacific and eastern atlantic oceans. *Biogeosciences*, 5(1), 171–201.

Strömborg, K. P., Smyth, T. J., Allen, J. I., Pitois, S., & O'Brien, T. D. (2009). Estimation of global zooplankton biomass from satellite ocean colour. *Journal of Marine Systems*, 78(1), 18–27.

Telszewski, M., Palacz, A., & Fischer, A. (2018). Biogeochemical in situ observations—motivation, status, and new frontiers. *New Frontiers in Operational Oceanography*, 131–160.

Volk, T., & Hoffert, M. I. (1985). Ocean carbon pumps: Analysis of relative strengths and efficiencies in ocean-driven atmospheric co2 changes. *The carbon cycle and atmospheric CO<sub>2</sub>: Natural variations Archean to present*, 32, 99–110.

Wakelin, S., Artioli, Y., Butenschön, M., Allen, J. I., & Holt, J. T. (2015). Modelling the combined impacts of climate change and direct anthropogenic drivers on the ecosystem of the northwest european continental shelf. *Journal of Marine Systems*, 152, 51–63.

Wakelin, S., Holt, J., Blackford, J., Allen, I., Butenschön, M., & Artioli, Y. (2012). Modeling the carbon fluxes of the northwest european continental shelf: Validation and budgets. *Journal of Geophysical Research: Oceans*, 117(C5).

Yu, Y., Si, X., Hu, C., & Zhang, J. (2019). A review of recurrent neural networks: Lstm cells and network architectures. *Neural computation*, 31(7), 1235–1270.

## Appendix A: Figures

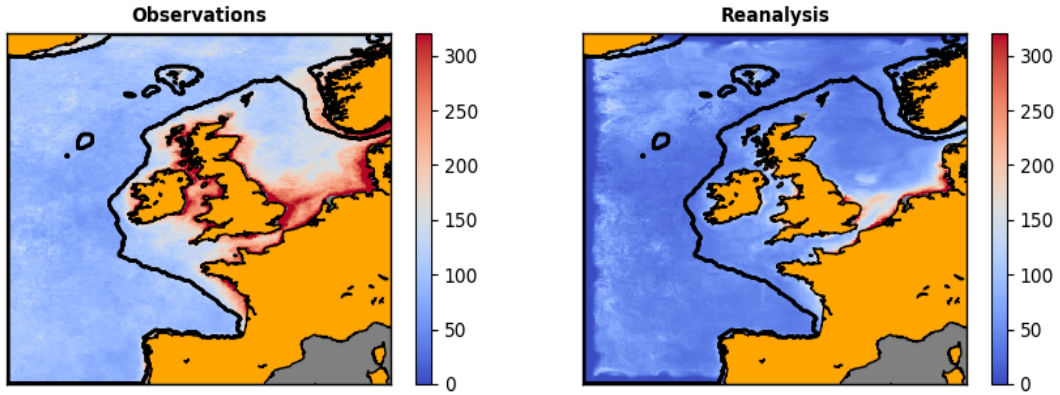


**Figure A1.** Comparing the Ocean Color (OC) - Climate Change Initiative (CCI) v4.2 satellite-derived product for total particulate organic carbon concentrations (in  $\text{mgC}/\text{m}^3$ ), broadly representing aggregate across phytoplankton, zooplankton, bacteria and detrital matter (left-hand panel), with the corresponding Copernicus reanalysis output (right-hand panel). The panels show temporally averaged values across the 2016-2017 period. The reanalysis was masked wherever there were missing satellite data, to ensure like-to-like comparison.

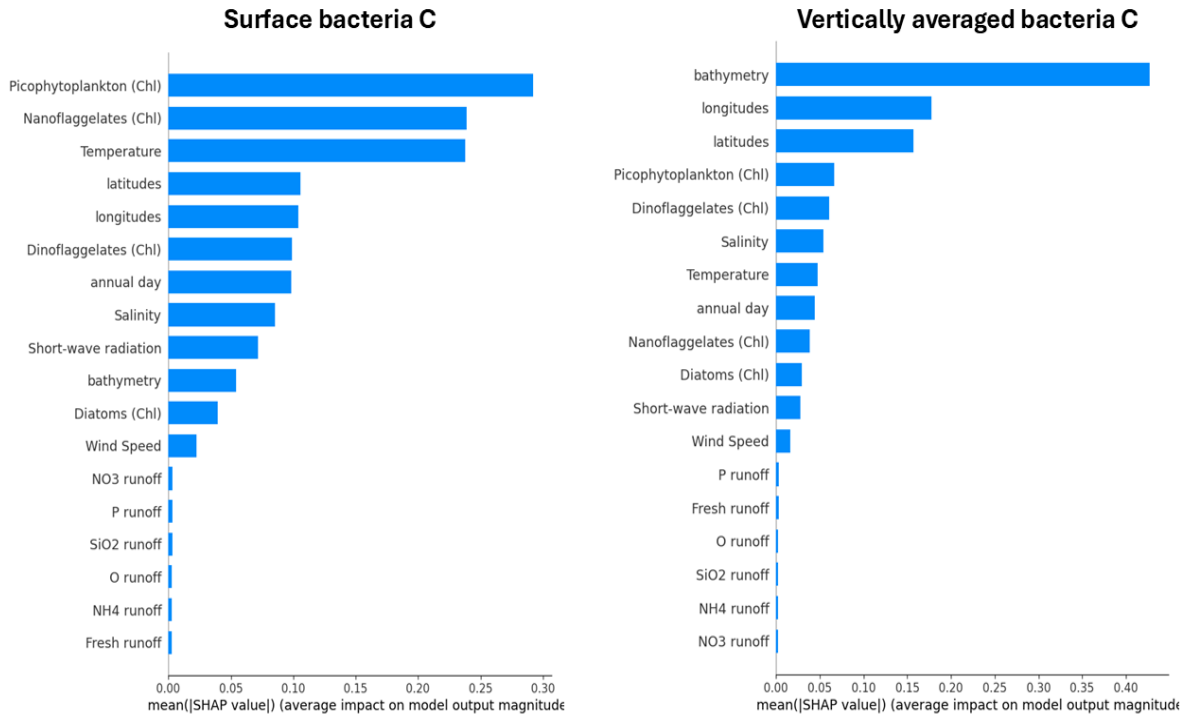


**Figure A2.** SHapley Additive exPlanations (SHAP) analysis (shown absolute values) for the surface heterotrophic bacteria carbon (left) and the vertically averaged heterotrophic bacteria carbon (right).

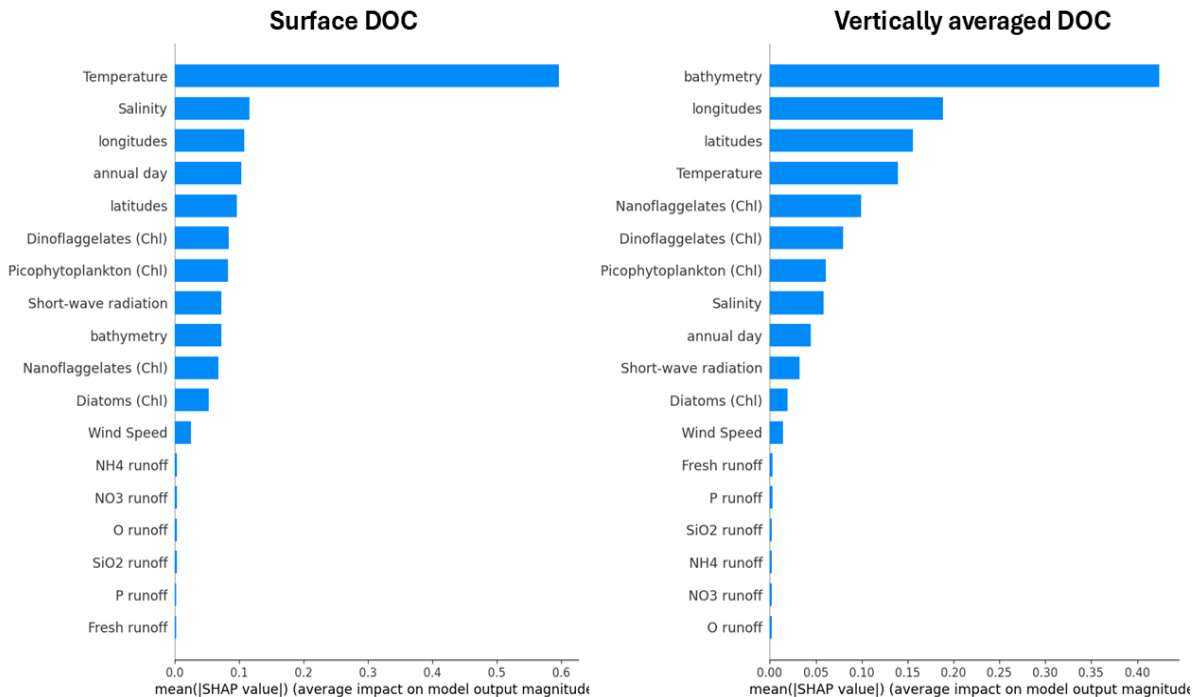


**Figure A3.** SHAP analysis (shown absolute values) for the surface dissolved organic carbon (DOC) (left) and the vertically averaged DOC (right).